APPROXIMATE ANALYTICAL MODELING OF CURRENT CROWDING EFFECTS IN MULTI-TURN SPIRAL INDUCTORS

William B. Kuhn
Department of Electrical and Computer Engineering, Kansas State University
Noureddin M. Ibrahim
Department of Electrical Engineering, Faculty of Engineering and Technology, Minia University, Egypt

ABSTRACT

The effective series resistance of a multi-turn spiral inductor operating at high frequencies is known to increase dramatically above its DC value due to proximity-effect or current crowding. This phenomenon is difficult to analyze precisely and has generally required electromagnetic simulation for quantitative assessment. Current crowding is studied in this work through approximate analytical modeling and first order expressions are derived for predicting resistance as a function of frequency. The results are validated through electromagnetic simulation and with measured data taken from a spiral inductor implemented in a Silicon-on-Sapphire process.

INTRODUCTION

Spiral inductors implemented in Silicon processes suffer from several power dissipation mechanisms, leading to poor inductor quality factors [1 - 5]. The best quality factors reported are generally achieved by etching away the underlying substrate [6], or by using very high resistivity or insulating bulk material [7]. In such cases, inductor Q's of 20 and above have been reported, with the highest values found in single turn spirals with correspondingly small inductance values of < 5nH. Unfortunately, for spirals with higher inductances, multiple turns are required and inductor Q often falls far short of the value that would be predicted from a simple calculation of inductor reactance divided by DC series resistance. This problem can be traced to an increase in effective resistance of the metal traces at high frequencies due to current crowding, with skin effect having only a marginal effect at low GHz frequencies [8 - 10].

Although the problem of current crowding is well known, little information is available in the literature to quantify it without resorting to numerical simulations [10]. In this paper we develop a first order analytical model of this effect and derive approximate formulas for predicting increases in effective series R with frequency. Our goal is to provide a framework for understanding the losses involved, and to develop simple expressions that can be used to guide explorations of the spiral inductor geometry design space without the need for repeated simulations or fabrication and characterization of many spirals. While some steps in the analysis currently rely on empirical expressions and others involve simple linearized approximations to higher order functions, the broad framework remains faithful to the physics involved and the predictions made by the model agree well with simulated and measured results.

MODEL DEVELOPMENT

The basic mechanism behind current crowding is illustrated in Figure 1. As the B field of adjacent turns in the inductor penetrates a trace normal to its surface, eddy currents are produced within the trace that add to the inductor's excitation current on the inside trace edge (nearest the center of the spiral) and subtract from (although actually in quadrature at low frequency) the excitation current on the outside edge. This "constricts" the current, increasing the effective resistance above the value that would exist for a uniform flow throughout the trace width.

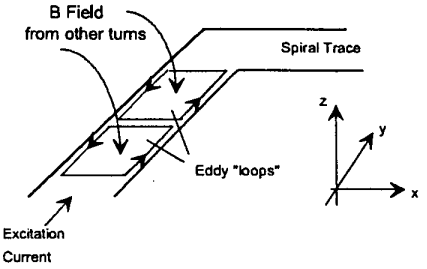

Figure 1. Illustration of current crowding.

A detailed analysis of this effect requires a sequence of steps including developing an expression for the normal B field, calculating eddy currents produced, computing power losses from these currents, and developing an effective resistance which accounts for the overall losses.

Normal B Field Distribution

Arguably, the most difficult analytical step is derivation of the B-field distribution within the inductor turns. In this paper, we bypass these difficulties by adopting the

0-7803-6280-2/00/$10.00 © 2000 IEEE

following empirical expression based on the results of finite element calculations for multi-turn spirals.

$$B(n) \approx B_o\left(\frac{n-M}{N-M}\right) \quad (1)$$

Here, n is the turn number for which the B field is computed (numbering from n=1 at the outside turn), $B(n)$ represents the average normal-directed B field within spiral turn n, N is the total number of turns, B_o is the average field at the inner-most turn (turn N), and M is the turn number where the field falls to zero and reverses direction.

Using finite element calculations of B, the following expression for B_o has been found to be reasonably accurate over a wide range of geometries.

$$B_o \approx 0.65\frac{\mu_o}{P} I_{ex} \quad (2)$$

In this expression, μ_o is the permeability of free space, P is the turn pitch, and I_{ex} is the excitation current. Values for M depend on the degree of spiral fill-in at the center, but a good estimate for typical multi-turn square or circular geometries with moderate fill is $M \approx \frac{N}{4}$.

Eddy Current Magnitude and Phase

At low frequencies, the induced E field responsible for the eddy current production follows Faraday's law, expressed in point form for the loop segment shown in Figure 1 as:

$$\nabla \times E \approx \frac{\partial E_y}{\partial x} = -j\omega B_z \quad (3)$$

which implies that the resulting eddy currents are actually in quadrature with the field and hence the excitation current. Integrating (3) with respect to x and approximating B as constant across trace n yields

$$E(x) = -j\omega B(n)\, x \quad \text{for } -W/2 \le x \le W/2 \quad (4)$$

and an eddy current density at the trace edges with a magnitude of

$$\left|J_{eddy}\right| = \sigma E = \sigma\, \omega B(n)\frac{W}{2} \quad (5)$$

where σ is the conductivity of the trace metal. Taking the ratio of (5) to the excitation current density in the trace of thickness T and combining with (2) then yields

$$\left|\frac{J_{eddy}}{J_{ex}}\right| = \frac{0.65}{2}\mu_o\, \sigma\, \omega\, T\, \frac{W^2}{P}\, \frac{(n-M)}{(N-M)} \quad (6)$$

This expression is maximum at the innermost turn ($n = N$), and if set to one for this case, can be used to find the frequency ω_{crit} at which the current crowding begins to become significant.

$$\omega_{crit} = \frac{3.1}{\mu_o}\frac{P}{W^2} R_{sheet} \quad (7)$$

Here, the trace's sheet resistance R_{sheet} has been used in place of $\frac{1}{\sigma T}$ to make the expression user friendly to the IC designer (and can be adjusted for skin effect if needed).

Field Redistribution at High Frequencies

The expressions derived above assume the B field within the inductor remains unchanged from the low frequency distribution assumed in Equation (1). At high frequencies, where eddy currents begin to become significant, this assumption must be checked.

For a multi-turn spiral, the field at turn n is the superposition of fields from all turns. Thus, while eddy currents flowing in adjacent turns will produce some modification to $B(n)$, the field contributions from equal and opposite eddy currents along the edges of other turns will largely cancel at turn n, and the net contribution from all turns will be relatively unchanged from that of uniform current for frequencies up to a few times ω_{crit}. For frequencies well above ω_{crit} however, the presence of large eddy currents along the edges of adjacent turns, and especially along the edges of turn n itself, can significantly change the field in turn n. One result is limiting of the eddy currents caused by back-EMF. This effect can be quantified approximately by treating the eddy current loops shown in Figure 1 as small inductances and finding the frequency where the reactance associated with the self inductance of the loop equals the resistance through which the eddy current flows. This yields the following estimate for the frequency where the limiting begins and the relationship between I_{eddy} and I_{ex} shifts to in-phase.

$$\omega_{\lim} \approx 18\, \frac{1}{\mu_o W} R_{sheet} \quad (8)$$

This is approximately 4 to 6 times ω_{crit} given in (7) for the case of spirals with $W \approx P$.

Resistance Increases with Frequency

Previous results can now be combined to approximate the effective series resistance R_{eff} of the spiral versus frequency. This can be done by setting $I_{ex}^2\, R_{eff}$ equal to the power dissipated. To simplify the analysis, we shall assume that the frequency of operation is below $\omega_{\lim}/2$ so that I_{ex} and I_{eddy} can be assumed to be in quadrature and the power dissipation from each can be computed independently. The power dissipated in the n'th turn is then:

$$P_n = I_{ex}^2 R_n + I_{eddy_n}^2 R_{eddy_n} \quad (9)$$

where R_n is the DC resistance of turn n and $R_{eddy\,n}$ is the resistance through which the eddy current $I_{eddy\,n}$ flows in turn n. R_n can be found from the sheet resistance R_{sheet} and the length of the turn l_n while $I_{eddy\,n}$ and the resistance R_{eddyn} through which it flows can be estimated by modeling the eddy current as being uniformly concentrated in regions of width W/4 along the spiral edges. Combining this approximation with (6) and (7), the following result is obtained:

$$P_n \approx I_{ex}^2 R_n \left[1 + \tfrac{1}{2}\left(\tfrac{\omega}{\omega_{crit}}\right)^2 \left(\tfrac{n-M}{N-M}\right)^2\right] \quad (10)$$

To find an expression for the total spiral resistance R_{eff}, (10) can be summed over n and the result equated to $I_{ex}^2 R_{eff}$ to give:

$$R_{eff} \approx R_{DC} + \tfrac{1}{2}\left(\tfrac{\omega}{\omega_{crit}}\right)^2 \sum_{n=1}^{N} R_n \left(\tfrac{n-M}{N-M}\right)^2 \quad (11)$$

where R_{DC} is the spiral's series resistance at DC and the terms within the summation are geometry dependent. Calculation of this sum for the typical case of a spiral with the inner third unfilled yields values in the range of 0.2 R_{DC} which can be used to give the following result for simple rough estimates of R_{eff}:

$$R_{eff} \approx R_{DC}\left[1 + \tfrac{1}{10}\left(\tfrac{\omega}{\omega_{crit}}\right)^2\right] \quad (12)$$

COMPARISON WITH MEASURED DATA

S11 data taken from a 9.5 nH inductor using Cascade Microtech coplanar waveguide probes connected to an HP8753A network analyzer are shown in Figure 2. The measurements are from a traditional square spiral with an outer dimension of 350um, N = 5.75, W = 18um, and P = 21um, fabricated in an SOS process with metal sheet resistance $R_{sheet} \approx 0.025$ Ohms/square (representing the effective value after stacking the three available metal layers). This data was fit to the model used in reference [11] consisting of a series R and L, with a capacitance C in parallel, and the value of C found was then removed from the impedance to extract the spiral's actual series inductance and resistance shown in Figure 3 from the apparent values measured. The virtually constant value of L vs frequency is used as a check on the fit of the model to the data throughout the frequency range. Inductor quality factor (computed as X_L/R) is also plotted, and shows the typical behavior seen in previously reported spirals.

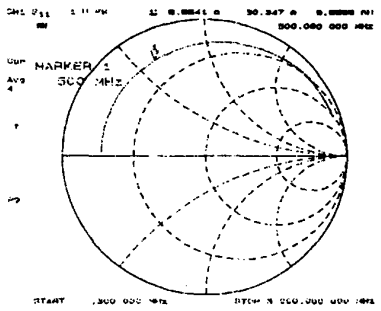

Figure 2. S11 measurements

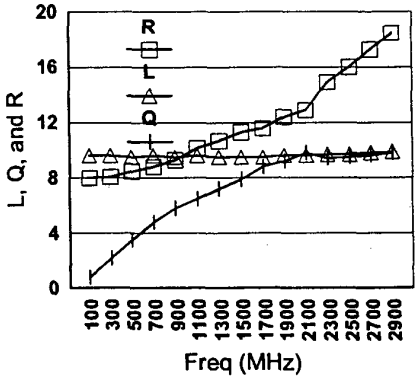

Figure 3. Measured parameters after fitting to lumped element model.

Comparison of values in Figure 3 to predictions of the analytic model show good agreement. Equation (7) predicts a critical frequency of 640 MHz for this spiral, while (12) predicts that the resistance will up by 10% at this frequency and rise at a quadratic rate. Figure 3 shows a resistance increase of 10% at approximately 700 MHz, and an increase of 40% at approximately two times this frequency, verifying both predictions. Equation (8) predicts that resistance increase will begin to level out in the neighborhood of 3 GHz, while the measured results show that the quadratic increase in resistance has slowed to linear by 2.9 GHz, the upper frequency range of measurement.

COMPARISON WITH SIMULATIONS

To validate the analytic model over a range of values for W, P, N, and R_{sheet} values, electromagnetic simulations were run with for the following cases (all have an outer dimension of 350um):

- Case 1: N = 6, W = 18um, P = 21um, and R_{sheet} = 0.028 Ohms/square [9.5 nH]
- Case 2: Same as case 1, but with R_{sheet} = 0.014 Ohms/square [9.5 nH]
- Case 3: Same as case 1, but with W decreased to 12um [9.4 nH]
- Case 4: N = 3, W = 38um, P = 42um, and Rsheet = 0.028 Ohms/square [2.6 nH]
- Case 5: Same as case 4, but with Rsheet increased to 0.056 Ohms/square [2.6 nH]
- Case 6: N = 12, W = 8.5um, P=10.5um, and Rsheet = 0.028 Ohms/square [35 nH]

For each case, the simulated S11 values were fit to the lumped element circuit model and the simulated series resistance versus frequency was found as described earlier. The results, expressed as resistance at frequency f divided by resistance at DC, are shown in Figure 4 and the predictions of critical frequency and limiting frequency from equations (7) and (8) for each case are shown in Table 1. The values of critical frequency from Table 1 agree well with the intercept points of the line R/Rdc = 1.1 as predicted by equation (12). In addition, all curves show the expected square-law behavior of resistance, and evidence of limiting at high frequency can be seen (although limiting does not follow predictions precisely).

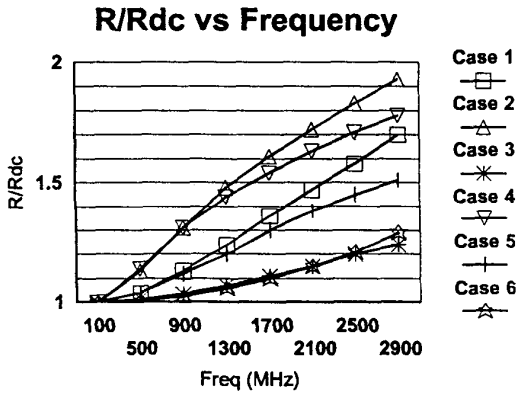

Figure 4. Spiral resistance divided by DC value for 6 different cases (see text).

Table 1. Predicted values of critical frequency and limiting frequency for 6 cases (see text).

Case	1	2	3	4	5	6
Critical f (MHz)	710	360	1,600	320	640	1,600
Limiting f (MHz)	2,500	1,800	5,300	1,700	3,400	7,500

SUMMARY AND CONCLUSIONS

Spiral inductors fabricated in processes with high resistivity substrates show significant increases in series resistance at high frequency. While the general mechanisms behind the current crowding mechanism responsible are well known, no simple quantitative expressions have been available to help in exploring the inductor design space. Equations (7), (8), and (12), derived in this work, provide reasonably accurate estimates for current crowding effects on series resistance of common multi-turn spirals. These expressions can be used to explore tradeoffs among spiral inductor parameters, to compute initial estimates of spiral performance, and to add first order modeling of current crowding effects to lumped element models used in circuit-level simulators.

ACKNOWLEDGEMENTS

This material is based on work supported by the National Science Foundation under Grant No. ECS-9875770. Spiral inductor fabrication was performed through MOSIS, and electromagnetic simulations were made possible by a donation of EDA tools from Agilent Technologies (formerly Hewlett Packard).

REFERENCES

[1] N. M. Nguyen, and R. G. Meyer, "Si IC-compatible inductors and LC passive filters," IEEE J. Solid-State Circuits, August 1990, pp. 1028-1031.

[2] C. P. Yue, C. Ryu, J. Lau, T. H. Lee, and S. S. Wong, "A Physical Model for Planar Spiral Inductors on Silicon," IEEE Int. Electron Devices Meetings, pp. 155 - 158, 1996.

[3] J. R. Long, M. A. Copeland, "The Modeling, Characterization, and Design of Monolithic Inductors for Silicon RF IC's," IEEE J. Solid-State Circuits, pp. 357-369, March 1997.

[4] W. B. Kuhn, and N. K. Yanduru, "Spiral Inductor Substrate Loss Modeling in Silicon RFICs," Microwave Journal, pp. 66 - 81, March 1999.

[5] J. N. Burghartz, M. Soyuer, and K. A. Jenkins, "Integrated RF and microwave components in BiCMOS Technology," IEEE Trans. Electron Devices, pp. 1559 - 1570, 1996.

[6] J. Y.-C. Chang, A. A. Abidi, and M. Gaitan, "Large Suspended Inductors on Silicon and Their Use in a 2-um CMOS RF Amplifier," IEEE Electron Device Letters, pp. 246-248, May, 1993.

[7] K. B. Ashby, I. A. Koullias, W. C. Finley, J. J. Bastek, and S. Moinian, "High Q Inductors for Wireless Applications in a Complementary Silicon Bipolar Process," IEEE J. Solid-State Circuits, pp. 4-9, Jan 1996.

[8] J. Craninckx and M. S. J. Steyaert, "A 1.8-GHz Low-Phase-Noise CMOS VCO Using Optimized Hollow Spiral Inductors," IEEE Journal of Solid-State Circuits, pp. 736 - 744, May, 1997.

[9] H-S. Tsai, J. Lin, R. C. Frye, K. L. Tai, M. Y. Lau, D. Kossives, F. Hrycenko, and Y-K. Chen, "Investigation of Current Crowding Effect on Spiral Inductors," IEEE MTT-S Int. Topical Symp. on Technologies for Wireless Applications, pp. 139 - 142, 1997.

[10] A. M. Niknejad, and R. G. Meyer, "Analysis, Design, and Optimization of Spiral Inductors and Transformers for Si RF IC's," IEEE J. Solid-State Circuits, pp. 1470 - 1481, Oct, 1998.

[11] R. A. Johnson, C. E. Chang, P. M. Asbeck, M. E. Wood, G. A. Garcia, and I. Lagnado, "Comparison of Microwave Inductors Fabricated on Silicon-on-Sapphire and Bulk Silicon," IEEE Microwave and Guided Wave Letters, pp. 323 - 325, Sept, 1996.